The Propagation potential

An Axonal response with implications for scalp-recorded EEG

A. P. Rudell and S. E. Fox
Department of Physiology, State University of New York Health Science Center at Brooklyn, Brooklyn, New York 11203 USA

ABSTRACT An electrophysiological response of axons, referred to as the "propagation potential," was investigated. The propagation potential is a sustained voltage that lasts as long as an action potential propagates between two widely spaced electrodes. The sign of the potential depends on the direction of action potential propagation. The electrode towards which the action potential is propagating is positive with respect to the electrode from which it is receding. For normal frog sciatic nerves the magnitude of the propagation potential was 17% of the peak of the extracellular action potential; TEA increased it to 32%. For normal earthworm median or lateral giant fibers it was 30%. A ripple pattern on the propagation potential was attributed to variation in resistance along the length of the worm. Cooling increased the duration of the propagation potential and attenuated the higher frequency components of the ripple pattern. Differential records from two widely spaced intracellular microelectrodes in the same axon differed from the propagation potential. The amplitude of the plateau relative to the peak was smaller, it decreased as the action potential propagated from one electrode site to the other, and the potential did not return to zero as rapidly as for extracellular records. When propagation was blocked by heat, the propagation potential slowly decayed. There was no ripple pattern during the decay. In a volume conductor, electrodes contacting the worm did not show the typical propagation potential, but electrodes located a few centimeters away from the worm did. Simple core-conductor models based on classical action potential theory did not reproduce the propagation potential. More complex, modified core-conductor models were needed to accurately simulate it. The results suggest that long, slowly conducting fibers can contribute to the scalp-recorded EEG.

INTRODUCTION

Extracellular microelectrode recordings of action potentials in brain typically have short durations, the order of one millisecond. It is argued here that this short duration is the result of a special recording configuration in which one electrode is close to the active membrane and the other is remote. The result is different for another configuration in which both of a pair of electrodes can be considered to be remote from the axonal membranes that support propagation of action potentials. In that case, the duration of the recorded potential can be quite long, depending on the distance between the recording electrodes and the velocity of action potential propagation.

We investigated this long duration potential, using excised frog sciatic nerves and single earthworm giant fibers. Widely spaced electrodes placed along the length of the axons recorded a steady potential component referred to here as the "propagation potential." The propagation potential was initially discovered during modeling of auditory brain-stem responses using frog sciatic nerves (Rudell, 1987). This property of actively conducting axons was of interest to us for two reasons. First, because its existence was surprising. It was not predicted by classical membrane theory (Hodgkin and Huxley, 1952). Second, the propagation potential had implications for the source of scalp-recorded EEG.

Early suggestions for the source of EEG waves pointed to activity in cortical neurons (Berger, 1929), specifically action potentials in cortical neurons (Adrian and Matthews, 1934*a*, *b*). Later, synaptic activity was suggested as the source (Eccles, 1951; Purpura, 1959). The frequency spectrum for EPSP's and IPSP's is close to that for EEG activity, and intracellular recordings of synaptic potentials are correlated with extracellularly recorded EEG waves (Klee et al., 1965; Creutzfeldt et al., 1966*a*, *b*). This and other supporting evidence led to general acceptance of the synaptic interpretation (Humphrey, 1968; Elul, 1972; Creutzfeldt and Houchin, 1974).

Action potentials usually are considered to be too short in duration and composed of a range of frequencies too high to be the source for spontaneous EEG activity. A number of studies, however, suggest that evoked responses which have very short latencies and durations may be produced by action potentials rather than synaptic activity. This was the conclusion reached for the auditory brain stem response (ABR) (Jewett et al., 1970; Caird et al., 1985; Sherg and Von Cramon, 1985; Rudell, 1987) and the somatosensory evoked potential (SEP) (Cracco and Cracco, 1976; Nakanishi et al., 1986). The long duration of the propagation potential is a feature of particular interest because it removes one of the arguments against action potentials as the

0006-3495/91/09/556/12 $2.00

source of spontaneous EEG activity and long latency, long duration evoked potential components.

The earthworm preparation was studied more extensively than the frog nerve preparation because it possessed a number of advantages. The principal one was that single fibers could be easily excited. Exciting only one axon avoided problems inherent in the compound response of whole nerves. First, whole nerves have a spectrum of different diameters, and therefore different conduction velocities. Second, all axons might not conduct the entire length of the nerve. The earthworm preparation had the additional advantage that median and lateral giant fibers could be independently excited. Thus, it was possible to study the effects of experimental manipulations on two types of fibers, one large diameter and rapidly conducting, the other smaller in diameter and more slowly conducting.

The giant axons of the earthworm are divided into segments by partitions called septa (Stough, 1930). The resistance across a septum is low, three orders of magnitude less than the plasma membrane (Brink and Barr, 1977; Brink and Fan, 1989). The low resistance is attributed to specialized junctional areas of plasma membrane called nexuses or gap junctions (Kensler et al., 1979). Conductance across the septal gap junctions is voltage independent (Kensler et al., 1979; Brink and Fan, 1989). In this respect they are like septal gap junctions in crayfish lateral axons, which are voltage-independent (Johnston and Ramon, 1982), but unlike the gap junctions between motor and lateral axons of the crayfish, which depend asymmetrically on transjunctional potential (Furshpan and Potter, 1957; Jaslove and Brink, 1986), or junctions found in the early embryos of some fish and amphibians (Spray et al., 1984).

The time delay in propagation across a septum is negligible, 150 μs (Kensler et al., 1979). These properties give the giant axons rapid, bidirectional action potential propagation (Eccles et al., 1933; Kao and Grundfest, 1957; Kao, 1960). They behave very much like nonseptated axons. The advantage conferred by the possiblity of recording single unit activity was considered to outweigh the disadvantage inherent in studying an axon that was atypical in being septate.

In an effort to understand the mechanism underlying the propagation potential we recorded intracellular potentials from giant fibers and constructed computer models. Simple core-conductor models could not reproduce all of the observed features of the propagation potential. More complex, modified core-conductor models were needed to match the recordings obtained from the biological preparations.

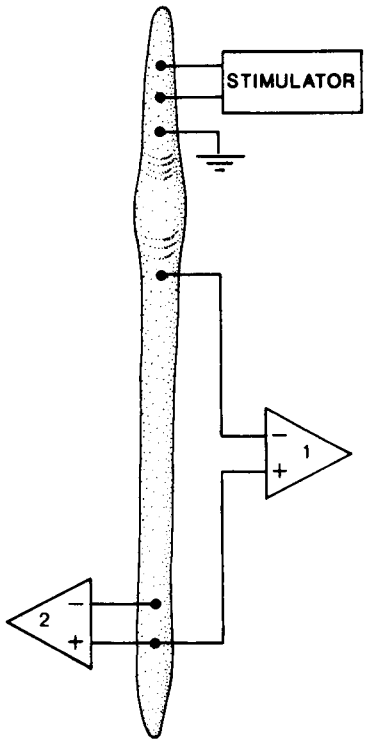

FIGURE 1 Stimulation and recording configuration for earthworms. A similar configuration was used for frog sciatic nerves. In that case the distal end of the sciatic nerve was stimulated.

METHODS

Frog sciatic nerves

After pithing, 10 to 12 cm lengths of sciatic nerve were removed from large bullfrogs (*Rana catesbeiana*). The nerves were stored temporarily in frog Ringer solution (Adrian, 1956). Later they were placed in a plexiglass tube that had electrodes embedded at regular intervals. The internal diameter of the tube was 5 mm. It was filled with frog Ringer and held in a vertical position with the distal end of the sciatic nerve near the top. The arrangement of stimulating and recording electrodes was similar to that used for the earthworm preparation (Fig. 1).

An upper pair of electrodes was used to stimulate the nerve through a constant current stimulus isolation unit. The distal end of the nerve was stimulated. This maximized the number of fibers that propagated action potentials the entire length of the nerve. (Proximal stimulation was not used because many of the axons that could be excited at that end would not traverse the entire length of the nerve. The drop out of fibers along the length of the nerve would be expected to produce decreased amplitude of the propagation potential with distance from the stimulation site.) Just below these leads an electrode grounded the preparation. A pair of electrodes further down, usually separated by 6 cm, was used for recording the compound action potential and the expected propagation potential.

The lower electrode of this pair and another electrode 1 cm higher formed a second recording channel. This channel was used to evaluate the possibility that beta fibers as well as alpha fibers were excited. For a 1 ms stimulus pulse an intensity of ~0.02 mA excited alpha fibers and a few beta fibers, as determined by the observation of two different

peaks. To avoid the complication of more than one group of fibers, stimulus intensity was set to a level below that at which beta fiber activity could be observed.

Grass P511 amplifiers were used with frequency settings at 1Hz and 10 KHz and appropriate gain for analog-to-digital conversion. The sampling rate was usually 13,750 Hz per channel, but it was reduced for experiments in the cold, when the conduction velocity was several times slower. Spectral analysis showed negligible power in the recording for frequencies above half the sampling rate, so aliasing was not a problem.

In most cases the liquid level in the tube was adjusted by syringe to lie between the stimulating and recording electrodes. In other cases the tube was completely drained or the normal Ringer solution was replaced by one containing 20 mM tetraethyl ammonium (TEA) (Hille, 1967).

Earthworm giant fibers

Earthworms were anesthetized with a 20% ethanol solution until they were immobile. Then stimulation and recording were carried out, either in the intact worm or on a dissected length of ventral nerve cord. Care had to be taken, using a dissecting scope, to preserve giant fibers that could conduct action potentials the entire length of the cord.

For intact worms there was often spontaneous activity, and electrical stimulation produced large potentials thought to be the responses of muscle fibers. They could be eliminated by greater time in the ethanol solution. This was done cautiously, because too much time in the ethanol could result in loss of the giant axon action potential response as well.

In a fresh worm the median giant fiber, about 100 μm in diameter, could be excited alone by a weak stimulus (0.5 mA, 1.0 ms). At several times this intensity both the median and the pair of smaller lateral giant fibers (~ 50 μm) could be excited. Action potential propagation failed after several hours. Usually the median giant fiber failed first, making it possible to test the lateral giant fibers alone.

For intracellular recording the dorsal half of the worm was removed. The edges of the ventral part were then trimmed to a distance of approximately 1 mm from the ventral cord. A thin transparent membrane was removed from a small area where the microelectrode was to penetrate. The electrodes were glass pipettes filled with 3 M KCl. They were driven by a micromanipulator at a shallow angle to the nerve fiber, ~ 20°. For recording in the cold the recording apparatus was surrounded by a jacket that could be filled with ice water. Using two micromanipulators, it was possible to record differentially between intracellular electrodes near the head and near the tail, but usually only one microelectrode recording was obtained.

Volume recording was done in a cylindrical glass tank, 14 cm in diameter. The tank was filled with 3 liters of earthworm Ringer (Kao and Grundfest, 1957). The earthworm was held vertically in the tank by a thin plastic rod. The part of the worm to be stimulated was held above the liquid level to decrease stimulus artifact. A pair of stainless steel recording electrodes contacted the earthworm on its ventral surface near the top and the bottom of the tank. A pair of Ag/AgCl recording electrodes were placed in the Ringer solution a few centimeters away from the worm near the top and the bottom of the tank. The amplitude of the response recorded from this latter pair was small, so a large number of responses had to be averaged. Testing was done in solutions of earthworm Ringer that were diluted from 0 to 100 times in different experiments.

Data analysis

For the purpose of combining results from different earthworms a normalization procedure was used to compensate for differences in amplitude and conduction velocity. The digital record was stretched or squeezed to a standard such that the number of digital points between the initial peak and the later trough was 100. The amplitude of the response was multiplied by a factor that produced a peak to trough amplitude of 1,000 U. Individual responses were then averaged with the digital record shifted so that the peak always occurred in the 64th bin and the trough in the 164th bin. Responses for 20 median giant and 20 lateral giant fibers were separately averaged.

The amplitude of the propagation potential for individual fibers was derived from the average of the central one half of the digital values between peak and trough, expressed as a percentage of the peak amplitude. The flatness of the plateau was estimated from the slope of the straight line that best fit the central one half points according to the method of least squares. Student's *t*-tests were calculated from these statistics to test the hypotheses that the amplitude of the propagation potential differed from zero and that the slope differed from zero.

Computer models

Mathematical models of action potentials propagating in unmyelinated axons were implemented on a computer (Cooley and Dodge, 1966). Such a core-conductor model of the earthworm median giant axon containing 100 compartments was constructed using PSPICE (MicroSim Corp., Irvine, CA) (Bunow et al., 1985). Inclusion of nonzero extracellular longitudinal resistance in each segment allowed the associated extracellular voltages to be determined for a one-dimensional conductive medium. Each compartment was 0.05 cm in length to give a total length of 5 cm for the axon model. Differences in voltage were measured between two extracellular nodes separated by several centimeters along the axon. In most cases a periaxonal compartment was interposed between the axon and the extracellular conductive medium. This compartment was bounded by the axon membrane on the inside and a "sheath" on the outside. The sheath was modeled by a radially oriented resistance, sometimes with a capacitance in parallel. The compartment lying between the axon membrane and the sheath was modeled by a longitudinal resistance.

The parameters for squid axons at 22°C (Hodgkin and Huxley, 1952) were adjusted to approximate the properties of the earthworm median giant fiber (Goldman, 1964). Axon diameter was set to 105 μm, axoplasmic resistivity to 200 ohm-cm, and membrane capacitance to 0.3 uF/cm^2. To match the membrane resistance to observed values (Goldman, 1964) the leak conductance and the voltage-dependent potassium conductance were reduced from those for squid by a factor of 0.28. To maintain stability a concurrent reduction in the maximum voltage-dependent sodium conductance ($\bar{g}_{Na}$) was required. A value of 50 mS/cm^2 for $\bar{g}_{Na}$ produced action potentials with rise-times and overshoots similar to those observed in real axons. The equilibrium potentials for the leak and the potassium conductances were adjusted to 0 and −5 mV, respectively. This minimized the hyperpolarizing afterpotential that is prominent in the squid and absent in the earthworm.

The simple core-conductor model described above did not produce a propagation potential. A more complex, modified core-conductor model was needed to produce flat plateaus having the correct polarity. The core-conductor model was "modified" by addition of a new feature. The new feature was a transient change in the longitudinal resistance of the periaxonal compartment with the passage of the action potential. This refinement was the only way we found to accurately approximate the waveforms recorded from real axons. The periaxonal resistance for the more complex computer model varied from 340 to 620 Kohms/cm, the variation being proportional to the derivative of the action potential. The resistance of the sheath in each compartment was taken as 200 Kohm (10 Kohm/cm). Extracellular resistance was set to 1 Kohm/cm.

RESULTS

Frog sciatic nerves

A typical response for a frog sciatic nerve is shown in Fig. 2. The inverting electrode, located nearer the stimulating leads, initially became negative with respect to the more distant electrode, producing a peak in the recording. This peak was followed by a plateau of the same sign, which continued for several milliseconds before a trough occurred. It is this plateau that we are calling the propagation potential. After the trough the potential difference rapidly returned to the zero level.

A propagation potential of the same sign as the initial peak was observed for every nerve tested. For eight frog sciatic nerves in normal Ringer the amplitude of the plateau averaged 17% of the peak amplitude. When the normal Ringer was replaced with Ringer containing TEA, the amplitude of the plateau gradually increased. Within an hour it had reached its maximum value. Then it averaged 32% of the peak amplitude. This increase was statistically significant ($t = 5.49, p < 0.001$).

Earthworm giant fibers

Intact worms

The results for the earthworm giant fibers were similar to those for frog sciatic nerves, but there were two important differences. The duration of the plateau was longer and it was more irregular, having a series of ripples throughout its duration (Fig. 3). The ripple pattern in a given preparation remained nearly the same for successive responses, but it differed from one worm to another. Thus, averaging responses for a number of different earthworms would be expected to attenuate the ripple pattern on the plateau, whereas averaging the responses for a given earthworm would not. When normalized responses for 20 median giant fibers were averaged, the plateau was much smoother. The same was true for an average of 20 lateral giant fibers (Fig. 4).

For the median giant fibers the propagation potential

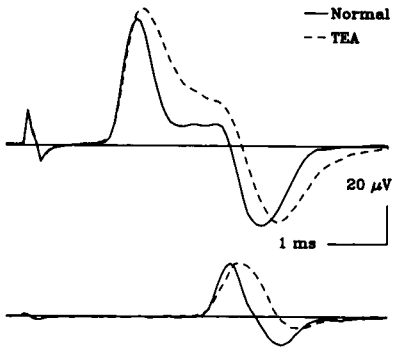

FIGURE 2 Frog sciatic nerve responses. The response of a frog sciatic nerve in a tube of normal frog Ringer solution (*solid line*) is superimposed on that recorded after the solution was replaced by Ringer solution containing TEA (*dashed line*). The widely separated pair of electrodes (interelectrode distance = 6 cm) recorded a plateau (the propagation potential) which became larger after treatment with TEA (*top*). The closely spaced distal electrodes (1 cm) showed a single peak (*bottom*), indicating the plateau was not due to a more slowly conducting fiber group. Each waveform is the average for 64 stimuli. The conduction velocity was 32 m/s. Calibration applies to both channels.

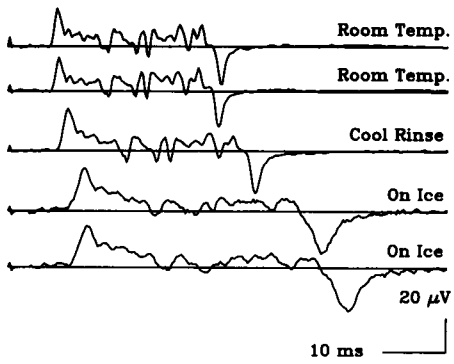

FIGURE 3 The effect of cooling on the propagation potential of earthworm lateral giant fibers. The responses were recorded from an intact, anesthetized worm in the air (interelectrode distance = 12 cm). Successive averages for 64 stimuli show nearly identical ripple structure on the plateau (*Top two responses*). Rinsing the worm in cool water increased the duration of the response, and preserved the ripple structure (*middle waveform*). Cooling on a bed of ice caused further increases in duration, with some attenuation of the ripple structure especially for the higher frequency components (*bottom two waveforms*). Conduction velocity was 4.7 m/s at room temperature. It decreased to 2.9 m/s for the lowest trace.

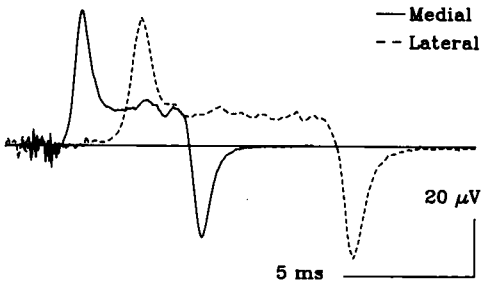

FIGURE 4 Normalized responses for earthworm giant fibers. The waveforms for 20 median giant fibers (*solid line*) and 20 lateral giant fibers (*dashed line*) are superimposed. The responses were recorded from intact worms in the air (interelectrode distance = 6 cm). The average conduction velocity was 12.9 m/s for median and 7.3 m/s for lateral giant fibers. The time calibration mark is based on the average time interval between peak and trough. The voltage calibration is based on the average of the peak-to-trough difference.

averaged 33% of the peak value. This value was significantly greater than zero ($t = 10.92, p < 0.001$). For the lateral giant fibers the average was 26%, also significantly different from zero ($t = 8.22, p < 0.001$), but not statistically different from the average for median giant fibers ($t = 1.51, p > 0.05$). The slope of the propagation potential did not differ from zero for the median fibers ($t = 0.12, p > 0.05$) or for the lateral fibers ($t = -0.86$, $p > 0.05$).

Bidirectional conduction

The sign of the propagation potential depended on the direction of propagation. The electrode towards which the action potential propagated was positive with respect to the electrode from which it receded. This rule applied for either direction of propagation, as illustrated for an intact worm in Fig. 5. The polarity observed when the head end was stimulated (Fig. 5, *top*) was opposite that observed when the tail end was stimulated (Fig. 5, *bottom*).

This result was confirmed in a group of 10 dissected fibers, five median and five lateral. The head end was stimulated followed a few seconds later by stimulation of the tail end, permitting examination of the propagation potential for either direction of conduction. In both cases the sign of the plateau was the same as the initial peak. The amplitude was not significantly different for the two directions of propagation ($t = 0.66, p > 0.05$) nor did the slopes differ ($t = 0.38$, $p > 0.05$). The sequence of ripples on the plateau for the caudal conduction was approximately the reverse order of that for rostral conduction. Correlation coefficients computed for the central one-half of the points between the peak and the trough for rostral conduction and a reversed sequence for caudal conduction were positive, ranging from 0.5 to 0.85.

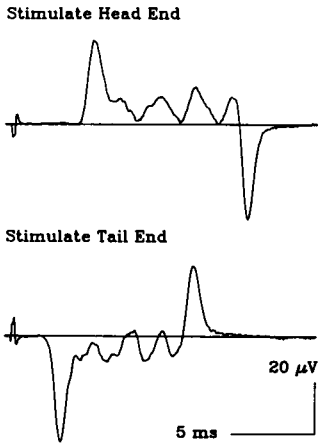

FIGURE 5 Propagation potentials for both directions of action potential propagation. The lateral giant fibers of an intact earthworm in air were excited by electrical stimulation at the head end. The response was recorded from widely spaced electrodes (interelectrode distance = 5 cm), producing the waveform shown at the top. Conduction velocity was 6.9 m/s. Later the tail end was stimulated, so the action potential propagated past the recording electrodes in the opposite direction (*bottom*). In both cases the propagation potential had the same sign as the initial peak. Each waveform is the average of 64 responses. The 20 microvolt calibration mark applies to both waveforms.

Varying extracellular resistance

The ripple pattern could be altered by local changes in resistance along the length of the worm. Resistance was decreased by laying a 1 cm length of stainless steel wire on the preparation. Resistance was increased by cutting a 1 cm notch in the dorsal side of the worm. For increased resistance there was an initial peak followed by a trough at the time the action potential was calculated to be traversing the notch. Just the opposite pattern was observed if the action potential traversed a region of decreased resistance, that is, an initial trough followed by a peak. The amplitude of these deflections could be quite large, even larger than the peak to trough amplitude normally recorded. If the local change was made nearer the stimulating leads the ripple occurred early; if further from them it occurred later.

Cold axons

Cooling the worm in an ice bath slowed conduction velocity as much as six times. The duration of the propagation potential was proportionately increased as were the peak and trough (Fig. 6). For some worms the

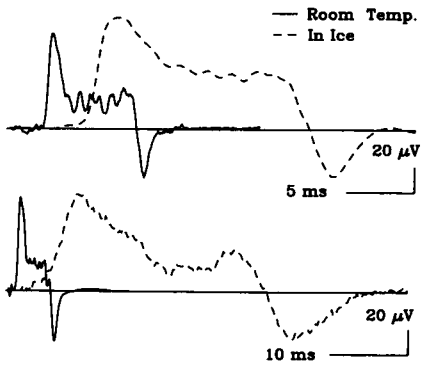

FIGURE 6 Earthworm giant fibers in the cold. Propagation potentials were recorded from median giant fibers in intact worms in air at room temperature (*solid line*) and ~1 h after being placed in an ice chamber (*dashed line*). The inter-electrode distance for the fiber response at the top was 8 cm. Conduction velocity was 11.8 m/s at room temperature, 5.0 m/s in ice. For the fiber response shown at the bottom, the interelectrode distance was 6 cm. Conduction velocity was 14.0 m/s at room temperature, 2.2 m/s in ice.

amplitude of the propagation potential in the cold was about the same as that for room temperature. For others it was larger, as much as 50% of the peak amplitude (Fig. 6, *top*). The ripple pattern on the plateau was attenuated, especially its higher frequency components.

Intracellular recordings

Intracellular recordings were taken from 12 median and four lateral giant fibers. Median and lateral fibers could easily be distinguished by their latency and threshold for excitation. Five median fibers and one lateral fiber were recorded with the worm at near zero temperature. The rest were recorded at room temperature. Spike amplitudes ranged from 60 to 95 mV. Depolarizing afterpotentials always followed the spike. In the cold the duration of the spike was several times longer than at room temperature (Fig. 7).

Differential recording of intracellular potentials from microelectrodes in the head and tail region of the same fiber showed a response that had some features in common with those of extracellularly recorded responses (Fig. 8). There were important differences. Of course, the amplitude was much larger and the polarity was reversed. Also, the relative size of the plateau with respect to the peak was less than that for recordings from extracellular electrodes, and the slope was not zero. No ripple pattern was seen on the plateau. After the action potential passed the second electrode the voltage did not return immediately to zero. The waveform of the intracellular differential recording could be accounted for by single algebraic addition of two intracellular recordings, with one of them inverted and lagged several milliseconds. These findings suggested that the observed intracellular plateaus represented a different phenomenon than the propagation potential.

Conduction block

In several worms conduction was reversibly blocked by heat. This could be done by applying radiance from a soldering iron held a few millimeters away from the worm. An alternative method was to dip a sealed tube containing the worm into a bath of warm water. By dipping the end of the worm distal to the stimulating leads into the bath several times, a temperature gradient was set up along the length of the worm, blocking conduction. Then when the worm was allowed to cool in the air, propagation would occur for increasingly greater lengths of the fiber until complete recovery occurred. When conduction was halted the propagation potential gradually decayed to zero (Fig. 9). There was no ripple pattern during the decay. The time course of decay was comparable to the time course for the afterpotentials of intracellular recording.

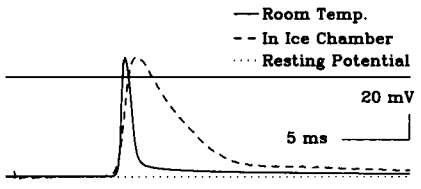

FIGURE 7 Intracellular recordings from earthworm median giant fibers. The intracellular response of a median giant fiber at room temperature (*solid line*) is superimposed on the response of another median giant fiber after cooling in an ice chamber (*dashed line*). Conduction velocity for the fiber at room temperature was 16.9 m/s. For the fiber in the cold it was 7.3 m/s.

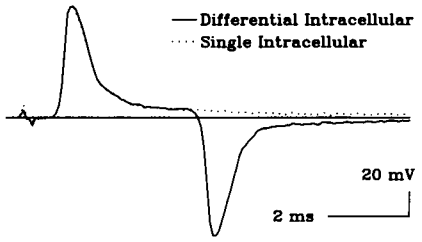

FIGURE 8 Single and differential intracellular recordings. The difference potential for one intracellular electrode in the head region and another in the tail region (*solid line*) is superimposed on the response for a single intracellular electrode in the head region (*dotted line*). The microelectrodes were separated 5.8 cm. Conduction velocity was 16.5 m/s. The resting potential of the single intracellular response was adjusted to zero to illustrate similarity.

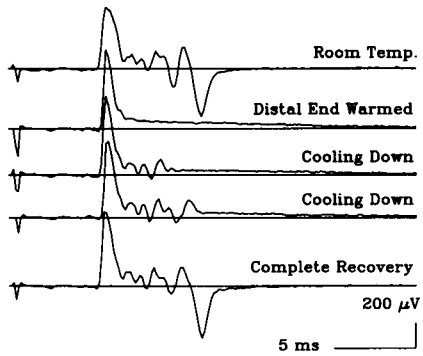

FIGURE 9 Earthworm lateral giant fiber conduction blocked by heat. The ventral cord was dissected and placed in a sealed recording tube. The response at room temperature is shown at the top. The interelectrode distance was 4 cm. Conduction velocity was 7.0 m/s. The distal end of the sealed tube was repeatedly dipped into a bath of warm water, until propagation failed just past the more proximal electrode (*second waveform*). The propagation potential decayed gradually. As the worm was allowed to cool in the air, the ripple pattern was extended (*third and fourth responses*). Complete recovery is shown at the bottom. The responses were not averaged. Only one stimulus was presented for each waveform.

Volume recording

When an earthworm was suspended in a tank of Ringer solution, widely spaced electrodes contacting the ventral surface of the worm did not show the typical plateau of the propagation potential. Instead the recording when the action potential was presumed to be propagating past the first recording electrode showed a triphasic waveform. This was followed by a slowly increasing ramp that nearly reached the level of the propagation potential just before a trough, which was considered to occur when the action potential propagated past the second electrode (Fig. 10, *top*). The amplitude of the entire waveform depended on the conductivity of the Ringer solution. Larger potential differences were recorded for more dilute, less conductive solutions.

By contrast, responses recorded with electrodes located several centimeters away from the worm were similar to those recorded when the worms were in air (Fig. 10, *second waveform*). The main difference was that the signals were much smaller and were generally noisier due to the high amplifier gain. To increase the signal-to-noise ratio many responses had to be averaged, particularly for nondiluted Ringer solution. In that case, the order of 1,000 responses had to be averaged to obtain a reasonably clear waveform.

For a group of 10 worms the propagation potential recorded by electrodes located several centimeters away from the worm was 22% of the peak amplitude, significantly greater than zero ($t = 4.93, p < 0.001$). The slope did not differ from zero ($t = 0.05, p > 0.05$). The very sharp, spikelike appearance of the peak and the trough (Fig. 11) was an artifact of the normalization method, caused by the much larger noise component in these records. If this effect was compensated for, the propagation potential was 30% of the peak amplitude, about the same that was observed for worms in the air.

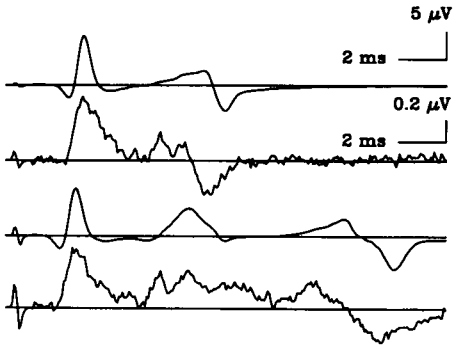

FIGURE 10 Responses of earthworm giant fibers in a volume conductor. The tail of an anesthetized, intact worm was held vertically in a tank of earthworm Ringer. The response of the median giant fiber, recorded from a pair of widely spaced electrodes (interelectrode distance = 6 cm) that contacted its ventral surface, is shown at the top. The corresponding response recorded from electrodes with similar spacing (5.8 cm), but removed from the worm 2.5 cm, is shown just below. When the stimulus intensity was increased, both median and lateral giant fibers were excited (*bottom two waveforms*). Conduction velocity was 10.2 m/s for the median fiber and 6.9 m/s for the lateral fibers. Each response is the average for 1,024 stimuli.

Computer models

The prominent depolarizing afterpotentials of earthworm giant axons could be modeled in space-clamped membrane by including the effect of potassium accumulation in the extracellular space (Adelman and Fitzhugh, 1975), but only when the effective thickness of the surrounding interstitial space was reduced to <100 Å. Attempts to include extracellular potassium accumulation in the 100 compartment PSPICE model were unsucessful due to the limited memory of the computer (6 Mb). Depolarizing afterpotentials could be modeled in the absence of potassium accumulation, but only when unrealistic parametric values were chosen. The values needed for the equilibrium potential for the leak and the equilibrium potential for potassium differed greatly from those inferred from observation (Goldman, 1964). The potential waveforms observed between intracellular points separated by several centimeters along the axon in this version of the model were similar to the differential intracellular records shown in Fig. 8.

The waveform of the extracellular potential changes for the core-conductor model with depolarizing afterpotentials was similar to the waveform of the intracellular potential changes, except for polarity and scaling. The extracellular waveform was smaller because the local circuit currents of the action potential flow through low resistances outside the axon, producing a small IR drop. The extracellular waveform of this model differed from that recorded from real axons in three ways. The

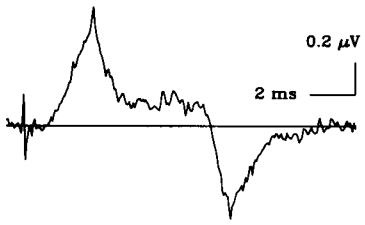

FIGURE 11 Normalized giant fiber responses in a volume conductor. The normalized response recorded from electrodes placed several centimeters away from the worm in a volume conductor is shown for ten giant fibers. The interelectrode distance was 6 cm. Conduction velocity averaged 10.0 m/s. The time calibration is based on the average interval between peak and trough. The voltage calibration is based on the average peak-to-peak amplitude.

peak/plateau ratio was smaller, the plateau was sloped, and the potential did not return rapidly to zero after the action potential had passed the second electrode site.

Variations in either intracellular or extracellular longitudinal resistance could produce ripples in the extracellular waveform similar to those recorded from extracellular electrodes in the earthworm. Such ripples did not occur in intracellular waveforms, even when intracellular longitudinal resistance changes were nearby. As for recordings from real axons, the amplitude of a ripple associated with a longitudinal resistance change could be even larger than the peak and trough associated with propagation of the action potential past the recording electrode sites.

A periaxonal compartment, interposed between the axon and the extracellular conductive medium, was added to the core-conductor model. This diminished the magnitude of the peak relative to that of the afterpotential. Although a peak/plateau ratio that conformed better to the peak/plateau ratio for real axons was produced by the addition of the periaxonal compartment, the magnitude of the slope of the plateau was not reduced, even with time constants for the sheath as long as 10 ms.

A fixed periaxonal resistance gradient along the entire length of the axon produced flat plateaus. The sign of the plateau depended on the direction of the resistance change, rather than the direction of action potential propagation. This conflicted with the results for real axons. For real axons, regardless of the direction of propagation, the polarity of the propagation potential was the same as the initial peak. Thus, simple compartmental models did not accurately generate the propagation potential.

Propagation potentials having the correct polarity could be produced by a modified core-conductor model in which *transient* changes in longitudinal resistance were associated with the passage of the action potential. Then propagation potentials were produced even in the absence of depolarizing afterpotentials (Fig. 12). In the compartmental PSPICE model a variable longitudinal resistance was included in the periaxonal space between the axon and the sheath. The value of this resistance varied in proportion to the derivative of the membrane voltage. This produced greater resistance in the region of the rising phase of the action potential and lower resistance in the region of the falling phase of the action potential. The derivative could be obtained either with respect to time or with respect to space, since conduction velocity was constant. In either case flat plateau voltages analogous to the propagation potential could be produced. The magnitude of the plateau depended on the degree to which resistance varied with the derivative of the action potential. To produce plateaus of the magnitude observed in real axons, the longitudinal resistance of the periaxonal compartment (base resistance of 420 Kohm/cm) needed to increase to a maximum of ~150% in the region of the rising phase of the action potential, and decrease to a minimum of 80% in the region of the falling phase.

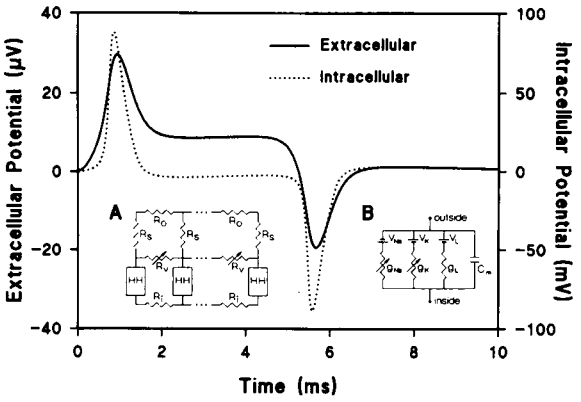

FIGURE 12 Intracellular and extracellular waveforms in axon models. The waveform recorded from intracellular electrodes separated by 3.5 cm (voltage inside compartment 10 minus voltage inside compartment 80) is plotted as a dotted line. Note the absence of depolarizing afterpotentials. Conduction velocity was 7.3 m/s at 22°C. Equally spaced extracellular electrodes recorded the propagation potential (voltage outside compartment 80 minus voltage outside compartment 10, *solid line*) only if the model contained a transient variation in longitudinal resistance associated with the action potential. (*A*) Equivalent circuit of the 100 compartment modified core-conductor model. Only compartments 1, 2, and 100 are illustrated. R_i is longitudinal resistance inside the axon. R_o is longitudinal resistance outside the sheath. R_v represents the variable periaxonal longitudinal resistance, whose value varies in proportion to the derivative of the action potential. R_s is the resistance of the "sheath." HH represents the nonlinear Hodgkin-Huxley-like model of the axon membrane. (*B*) Equivalent circuit of the Hodgkin-Huxley-like model. V_{Na}, V_K, and V_L represent the equilibrium potentials for Na^+, K^+, and the leak, respectively. g_{Na}, g_K, and g_L represent the conductances for the same ionic species. C_m is membrane capacitance for a compartment. For the modified core-conductor model illustrated in *A*, the "outside" terminal was connected to the periaxonal compartment.

DISCUSSION

The existence of the propagation potential

The issues addressed in the discussion section present the most certain conclusions first, followed by those of a more speculative nature. The most certain conclusion reached is that the propagation potential exists. Until recently we were not aware of any other reports that illustrated responses similar to the propagation potential, but we were convinced of its existence because of its

consistant appearance under a wide variety of conditions. The failure to find comparable responses in the literature was attributed to insufficient axon length or inappropriate recording configurations. Then we noticed that the frog sciatic nerve responses shown by Deupree and Jewett (1988), illustrated in their Fig. 2, were strikingly similar to our own recordings. The responses were recorded from widely separated electrodes in a volume conductor filled with Ringer's solution. The length of nerve that extended into the volume was sufficiently long (8 cm) to make a plateau evident between the initial peak and the subsequent trough. It had the correct polarity and was about one-fourth to one-fifth as large as the initial peak. The authors did not comment on this feature of their responses, but it is likely that it is the same phenomenon that we investigated in this study. Thus, there is some independent support of our findings for normal frog sciatic nerves.

The propagation potential was present for both the sciatic nerve and the earthworm preparations. This finding blunted criticism that might have been appropriate for one preparation, but not the other. The frog sciatic nerve preparation contained no muscle fibers or septate axons. The earthworm responses were produced by single axons, not the compound of many action potentials. That the propagation potential could be observed for axons as different as those for the earthworm and the frog, one septate, the other myelinated and nonseptate, suggests that it is a feature of axons generally, and not unique to those used as models in this study.

The ripple pattern

Far-field recordings of action potentials show stationary peaks that have been attributed to electric inhomogeneity (Nakanishi, 1982; Scherg and Von Cramen, 1985) changes in the shape of the volume conductor (Kimura et al., 1984) and bends in the course followed by the nerve fibers in a volume conductor (Nakanishi et al., 1986; Rudell, 1987; Deupree and Jewett, 1988). The ripple pattern observed on the plateau is best explained by variation in extracellular resistance along the length of the worm. Manipulation of local extracellular resistance gave results consistent with those described by others in the context of stationary peaks (Desmedt et al., 1983; Nakanishi, 1983; Eisen et al., 1986; Kimura et al., 1986; Stegeman et al., 1987).

It is unlikely that the ripple pattern was due to the septa or variations in the extracellular conductivity near the septa or ganglia. The interseptal distance is ~1 mm (Brink and Dewey, 1978; Brink and Fan, 1989). Thus, for the usual 6 cm interelectrode distance, about 60 septa would have been traversed, which should have produced a corresponding number of ripples. This figure is about 10 times greater than the number of ripples actually observed.

The attenuation of high frequency components of the ripple pattern observed when axons were cooled can be explained by the greater wavelength of action potentials in the cold. By integrating resistance changes over a longer length, the resistance profile was smoothed. This process is similar to a method of digital filtering sometimes used, called the "running average." A greater degree of smoothing is obtained if the number of successive samples in the running average is increased.

The ripple pattern recorded by the distant extracellular electrodes "read out" changes in longitudinal resistance as the action potential propagated along the axon. Because the resistance profile along the axon was fixed, the pattern read out for one direction of propagation was approximately the reverse of the pattern read out during propagation in the opposite direction. The pattern was not exactly the reverse because the action potential was asymmetric in time, and therefore also in space. The asymmetry was characterized by the action potential having a sharper rise time than fall time. Instead of the rectangular window used for the running average, the window of integration had the shape of the action potential.

When propagation was halted midway along the axon, the extracellular plateau gradually decayed. During the decay there was no ripple pattern. This result was consistent with the idea that the action potential was no longer propagating, and because it was not moving in space, it ceased to read out new extracellular resistance values along the length of the axon.

The ripple pattern was not seen in the intracellular records of either real axons or computer models, even when the recordings were differential. This reflects a fundamental difference between the two recording methods, the intracellular recordings showing only local membrane potential changes, the extracellular capable of recording the effects of the local circuit currents of action potential propagation from a distance of several centimeters.

The existence of the propagation potential seems firmly established, and a satisfactory explanation for the ripple pattern riding on it has been given. The mechanism for production of the propagation potential, however, and its implications for EEG recording are more controversial issues now to be addressed.

The mechanism of the propagation potential

Both frog (Barrett and Barrett, 1982) and earthworm giant fibers (Kao and Grundfest, 1957) are known to

have depolarizing afterpotentials, as do most axons. These afterpotentials have durations as long as several hundred milliseconds, so they might be thought to be responsible for the propagation potential. Further analysis indicated this explanation was unlikely.

For widely spaced electrodes the extracellularly recorded potential is not a simple mirror image of the differentially recorded intracellular potential. The intracellular plateau of the depolarizing afterpotentials is not flat, but continuously decreases, and after the action potential has propagated past the second electrode, the return to zero is not as rapid as it is for extracellular recording. The peak/plateau ratio is smaller for the intracellular than for the extracellular records. As shown by computer modeling, these differences cannot be explained by a simple low pass filtering effect of the surrounding tissue.

The steady potential observed when an action potential propagates between two extracellular recording electrodes implies a voltage drop due to longitudinal current flows. The currents are the local circuit currents associated with action potential propagation. Given constant intracellular longitudinal resistance as a function of distance in a core-conductor model, the two intracellular longitudinal currents associated with the rising and the falling phases of the action potential are equal and opposite. This must be true because the values of the intracellular potential before and after the action potential are identical. In addition, the intracellular and extracellular longitudinal current flows for each loop must be equal and opposite, because the total membrane current must be zero. So, the two extracellular longitudinal currents associated with the rising and falling phases of the action potential must also be equal and opposite. Therefore, a propagation potential in the core-conductor model could not be produced by differences in net current flow in the forward and reverse loops, but must be produced by different voltage drops across impedances in the paths for the local circuit current flow. This conclusion applies only to the core-conductor model. In a volume conductor, the possible current paths are more complex, so other explanations that do not require impedance differences might account for voltage plateaus.

The computer models of core-conductors showed that a flat plateau was produced if the periaxonal longitudinal resistances were asymmetric about the peak of the action potential. Results from models that used a fixed resistance gradient along the length of the axon could not account for the results obtained for the bidirectional conduction experiments in real axons. To accurately reflect the results in real axons, it was necessary to assume that the longitudinal resistance gradient depended on the direction of propagation. A plateau of the proper polarity was produced if the ratio of the extracellular longitudinal resistance in the region of the rising phase of the action potential to the corresponding resistance in the region of the falling phase was greater than one. Such a transient longitudinal resistance gradient could be produced by causing the resistance in the periaxonal space to vary in proportion to the derivative of the membrane voltage. Then the modified core-conductor model produced responses that closely approximated those observed in the biological preparations. The plateau was flat and the voltage returned rapidly to zero after the action potential passed the second electrode. The peak/plateau ratio could be adjusted to empirical values by varying the factor for resistance change per action potential derivative value. The success of this model did not depend on a depolarizing afterpotential. No afterpotential was necessary. This gave additional support for the conclusion that the afterpotential itself was not responsible for producing the propagation potential in real axons.

In the modified core-conductor model the periaxonal resistance was varied in proportion to the derivative of the membrane potential. This does not necessarily imply a voltage-dependent conductivity of the medium just outside the membrane. Aftereffects of the passage of the action potential other than the transmembrane potential might be responsible for the resistance change. In that case, the transmembrane potential would only serve as an index of the passage of the action potential, rather than being a causative factor as it is for Na^+ and K^+ conductances across the membrane. For example, swelling of the axolemma-ectoplasm complex during an action potential, as proposed by Tasaki and Byrne (1990), might alter the longitudinal resistance of the periaxonal compartment. Changes in extracellular ionic concentrations might also influence longitudinal resistance.

The amplitude of the propagation potential was significantly enhanced by TEA, which blocks K^+ conductance. This suggests that transmembrane ionic flows are involved in the mechanism. Blocking K^+ conductance might produce a greater longitudinal resistance gradient because it reduces the quantity of K^+ released with each action potential. In the modified core-conductor model, an increase in the amplitude of the propagation potential required a larger than normal ratio of extracellular resistance in the region of the rising phase to the extracellular resistance in the region of the falling phase. K^+ accumulation in the extracellular space seems an unlikely explanation for the generation of the propagation potential. If the propagation potential were caused directly by extracellular accumulation of K^+, the TEA would have been expected to *reduce* its amplitude, not increase it, because TEA reduces K^+ release.

There is little evidence in real axons for transient changes in longitudinal resistance such as those employed in the modified core-conductor model. We dislike appealing to such a hypothetical process, but an assumption of this sort was the only way we found to obtain behavior from the core-conductor model that accurately reflected what was observed for real axons. The experiments reported here are suggestive, but further research is necessary to establish firmly a detailed account of the mechanism responsible for production of the propagation.

The propagation potential as a source for the EEG

Scalp-recorded electrical activity may have a different source than that for activity recorded from electrodes placed in the brain itself. In a "near" recording configuration an "active" electrode is placed in the brain near the membranes that govern neuronal current flow. A 30 μm difference in location can result in radically different patterns of spontaneous brain waves (Elul, 1972). The location of the reference electrode is relatively unimportant. It could be moved so that the vector defined by the location of the two recording electrodes changed 90° without substantially affecting the response.

In a "remote" recording configuration where the electrodes are placed on the scalp, neither is near the neuronal membranes. For widely spaced electrodes, either could be moved a centimeter without radically changing the brain wave signal recorded (Spitzer et al., 1989). The vector defined by the location of the two electrodes is more important for the remote than for the near configuration. Substantial changes in the recorded signal can occur if the vector is changed by 90° (Rudell, 1987). Our suggestion that action potentials propagating in long axons contribute to EEG waves is limited to recording in the remote configuration.

The response of a single axon recorded from remotely placed leads in a volume of saline integrated to a non-zero sum (over the duration of propagation). The initial peak and subsequent trough were nearly equal, but opposite in sign, leaving only the plateau to produce the non-zero sum. Integration to a non-zero sum is important because it allows summation of the activity of individual axons, even when synchronization is not precise. Cancellation of peaks and troughs may occur because of their opposite sign, but action potentials propagating in the same direction produce plateaus of the same polarity, which should summate rather than cancel.

The amplitude of the propagation potential should depend on the impedance of the brain. The volume recording experiment showed the response was larger when the axons were in a high impedance medium. Low frequency impedance in the brain is 5–10 times higher than that for a physiological saline solution (Ranck, 1963; Nicholson, 1965; Hoeltzell and Dykes, 1979). Impedance is higher for low than for high-frequency signals because the current mostly flows in the narrow extracellular spaces, not crossing high-resistance membranes to an appreciable extent (Elul, 1972).

The principles learned from study of the propagation potential suggest the following might be important factors for scalp-recorded responses. (*a*) Axons whose course parallels the vector defined by the electrode locations should contribute more to the record than transversely oriented axons. (*b*) Long axons that propagate action potentials slowly should contribute more to the record than short rapidly conducting axons because (1) longer duration responses integrate to a larger sum and (2) the impedance of the brain is higher for low-frequency signals than for high. (*c*) A majority of action potentials should be propagating in the same direction. An equal number of action potentials conducting in opposite directions at the same time should produce cancelling and little or no effect on the record.

This work was supported in part by Campus Research Development Fund grant 412-9375 B to A. P. Rudell and National Institute of Health grant NS17095 to S. E. Fox.

Received for publication 3 January 1990 and in final form 23 April 1991.

REFERENCES

Adelman, W. J., Jr., and R. Fitzhugh. 1975. Solutions of the Hodgkin-Huxley equations modified for potassium accumulation in a periaxonal space. *Federation Procceedings.* 34:1322–1329.

Adrian, R. H. 1956. The effect of internal and external potassium concentration on the membrane potential of frog muscle. *J. Physiol. (Lond.).* 133:631–658.

Adrian, E. D., and B. H. C. Matthews. 1934*a*. The Berger rhythm: potential changes from the occipital lobes in man. *Brain.* 57:355–385.

Adrian, E. D., and B. H. C. Matthews. 1934*b*. The Interpretation of potential waves in the cortex. *J. Physiol. (Lond.).* 81:440–471.

Barrett, E. F., and J. N. Barrett. 1982. Intracellular recording from vertebrate myelinated axons: mechanism of the depolarizing afterpotential. *J. Physiol. (Lond.).* 323:117–144.

Berger, H. 1929. Uber das Elektrenkephalogramm des Menschen. *Arch. Psychiatr. Nervenkr.* 87:527–570.

Brink, P. R., and L. Barr. 1977. The resistance of the septum of the median giant axon of the earthworm. *J. Gen. Physiol.* 69:517–536.

Brink, P. R., and M. M. Dewey. 1978. Nexal membrane permeability to anions. *J. Gen. Physiol.* 72:69–86.

Brink, P. R., and S. Fan. 1989. Patch clamp recordings from membranes which contain gap junction channels. *Biophys. J.* 56:579–593.

Bunow, B., I. Segev, and J. W. Fleshman. 1985. Modeling the electrical behavior of anatomically complex neurons using a network analysis program: excitable membrane. *Biol. Cybern.* 53:41–56.

Caird, D., D. Sontheimer, and R. Klinke. 1985. Intra- and extracranially recorded auditory evoked potentials in the cat. I. source location and binaural interaction. *Electroencephalogr. Clin. Neurophysiol.* 61:50–60.

Cooley, J. W., and F. A. Dodge, Jr. 1966. Digital computer solutions for excitation and propagation of the nerve impulse. *Biophys. J.* 6:583–599.

Cracco, R. Q., and J. B. Cracco. 1976. Somatosensory evoked potential in man: far field potentials: *Electroencephalogr. Clin. Neurophysiol.* 41:460–466.

Creutzfeldt, O., and J. Houchin. 1974. Neuronal basis of EEG waves. *In* Handbook of Electroencephalography and Clinical Neurophysiology. A. Remond, and O. Creutzfeldt, editors. Elsevier Science Publishers B. V., Amsterdam. 2A5–2A55.

Creutzfeldt, O., S. Watanabe, and H. D. Lux. 1966*a*. Relations between EEG phenomena and potentials of single cortical cells I. Evoked responses after thalamic and epicortical stimulation. *Electroencephalogr. Clin. Neurophysiol.* 20:1–18.

Creutzfeldt, O., S. Watanabe, and H. D. Lux. 1966*b*. Relations between EEG phenomena and potentials of single cortical cells II. Spontaneous and convulsoid activity. *Electroencephalogr. Clin. Neurophysiol.* 20:19–37.

Desmedt, J. E., N. T. Huy, and J. Carmeliet. 1983. Unexpected shifts of the stationary p9 somatosensory evoked potential far field with changes in shoulder position. *Electroencephalogr. Clin. Neurophysiol.* 56:628–634.

Deupree, D. L., and D. L. Jewett. 1988. Far-field potentials due to action potentials traversing curved nerves, reaching cut nerve ends, and crossing boundaries between cylindrical volumes. *Electroencephalogr. Clin. Neurophysiol.* 70:355–362.

Eccles, J. C. 1951. Interpretation of action potentials evoked in the cerebral cortex. *Electroencephalogr. Clin. Neurophysiol.* 3:449–464.

Eccles, J. C., R. Granit, and J. Z. Young. 1933. Impulses in the giant fibers of earthworms. *J. Physiol.* (*Lond.*). 77:23P–24P.

Eisen, A., K. Odusote, C. Bozek, and M. Hoirch. 1986. Far-field potentials from peripheral nerve: generated at sites of muscle mass change. *Neurology.* 36:815–818.

Elul, R. 1972. The genesis of the EEG. *Int. Rev. Neurobiol.* 15:227–272.

Furshpan, E. J., and D. D. Potter. 1957. Mechanism of nerve-impulse transmission at a crayfish synapse. *Nature* (*Lond.*). 180:342–343.

Goldman, L. 1964. The effects of stretch on cable and spike parameters of single nerve fibers: some implications for the theory of impulse propagation. *J. Physiol.* (*Lond.*). 175:425–444.

Hille, B. 1967. The selective inhibition of delayed potassium current in nerve by tetraethylammonium ion. *J. Gen. Physiol.* 50:1287–1302.

Hodgkin, A. L., and A. F. Huxley. 1952. A quantitative description of membrane currents and its application to conduction and excitation in nerve. *J. Physiol.* (*Lond.*). 117:500–544.

Hoeltzell, P. B., and R. W. Dykes. 1979. Conductivity in the somatosensory cortex of the cat—evidence for cortical anisotrophy. *Brain Res.* 127:61–82.

Humphrey, D. R. 1968. Reanalysis of the antidromic response. II On the contribution of cell discharge and PSP's to the evoked potential. *Electroencephalogr. Clin. Neurophysiol.* 25:421–442.

Jaslove, S. W., and P. R. Brink. 1986. The mechanism of rectification at the electronic motor giant synapse of the crayfish. *Nature* (*Lond.*). 323:63–65.

Jewett, D. L., M. N. Romano, and J. S. Williston. 1970. Human auditory evoked potentials: possible brain stem components detected on the scalp. *Science* (*Wash. DC*). 167:1517–1518.

Johnston, M. F., and F. Ramon. 1982. Voltage independence of an electrotonic synapse. *Biophys. J.* 39:115–117.

Kao, C. Y. 1960. Postsynaptic electrogenesis in septate giant axons. II. Comparison of medial and lateral giant axons of crayfish. *J. Neurophysiol.* (*Bethesda*). 23:618–635.

Kao, C.Y., and H. Grundfest. 1957. Postsynaptic electrogenesis in septate giant axons. I. Earthworm median giant axon. *J. Neurophysiol.* (*Bethesda*). 20:553–573.

Kensler, R. W., P. R. Brink, and M. M. Dewey. 1979. The septum of the lateral axon of the earthworm: a thin section and freeze-fracture study. *J. Neurocytol.* 8:565–590.

Kimura, J., A. Mitsudome, T. Yamada, and Q S. Dickins. 1984. Stationary peaks from a moving source in far-field recording. *Electroencephalogr. Clin. Neurophysiol.* 58:351–361.

Kimura, J., A. Kimura, T. Ishida, Y. Kudo, S. Suzuki, M. Machida, H Matsuoka, and T. Yamada. 1986. What determines the latency and amplitude of stationary peaks in farfield recordings? *Ann. Neurol.* 19:479–486.

Klee, M. R., K. Offenlock, and J. Tigges. 1965. Cross-correlation analysis of electroencephalographic potentials and slow membrane transients. *Science* (*Wash. DC*). 147:519–521.

Nakanishi, T. 1982. Action potentials recorded by fluid electrodes. *Electroencephalogr. Clin. Neurophysiol.* 53:343–345.

Nakanishi, T. 1983. Origin of action potential recorded by fluid electrodes. *Electroencephalogr. Clin. Neurophysiol.* 55:114–115.

Nakanishi, T., M. Tamaki, and K. Kudo. 1986. Possible mechanism of generation of SEP farfield component in the brachial plexus in the cat. *Electroencephalogr. Clin. Neurophysiol.* 63:68–74.

Nicholson, P. W. 1965. Specific impedance of cerebral white matter. *Exp. Neurol.* 13:386–401.

Purpura, D. P. 1959. The nature of electrocortical potentials and synaptic organizations in cerebral and cerebellar cortex. *Int. Rev. Neurobiol.* 1:47–163.

Ranck, J. B., Jr. 1963. Specific impedance of rabbit cerebral cortex. *Exp. Neurol.* 7:144–152.

Rudell, A. P. 1987. A fiber tract model of auditory brain-stem responses. *Electroencephalogr. Clin. Neurophysiol.* 67:53–62.

Scherg, M., and D. Von Cramon. 1985. A new interpretation of the generators of BAEP waves I-V: results of spatio-temporal dipole model. *Electroencephalogr. Clin. Neurophysiol.* 62:290–299.

Spitzer, A. R., L. G., Cohen, J. Fabrikant, and M. Hallett. 1989. A method for determining optimal interelectrode spacing for cerebral topographic mapping. *Electroencephalogr. Clin. Neurophysiol.* 72:355–361.

Spray, D. C., R. L. White, A. Carvalho, A. L. Harris, and M. V. L. Bennett. 1984. Gating of gap junction channels. *Biophys. J.* 45:219–230.

Stegeman, D. F., A. Van Oosterom, and E. J. Colon. 1987. Far-field evoked potential components induced by a propagating generator: computational evidence. *Electroencephalogr. Clin. Neurophysiol.* 67: 176–187.

Stough, H. B. 1930. Polarization of the giant fibers of the earthworm. *J. Comp. Neurol.* 50:217–229.

Tasaki, I., and P. M. Byrne. 1990. Volume expansion of nonmyelinated nerve fibers during impulse conduction. *Biophys. J.* 57:633–635.